Registration of X-ray mammograms and three-dimensional speed of sound images of the female breast

Torsten Hopp[a], Marie Holzapfel[a], Nicole V. Ruiter[a], Cuiping Li[b] and Neb Duric[b]

[a]Karlsruhe Institute of Technology, Institute for Data Processing and Electronics, Karlsruhe, Germany;
[b]Barbara Ann Karmanos Cancer Institute, Department of Radiation Oncology, Detroit, USA

ABSTRACT

Breast cancer is the most common type of cancer among women in Europe and North America. The established screening method to detect breast cancer is X-ray mammography, although X-ray frequently provides poor contrast for tumors located within glandular tissue. A new imaging approach is Ultrasound Tomography generating three-dimensional speed of sound images. This paper describes a method to evaluate the clinical applicability of three-dimensional speed of sound images by automatically registering the images with the corresponding X-ray mammograms. The challenge is that X-ray mammograms show two-dimensional projections of a deformed breast whereas speed of sound images render a three-dimensional undeformed breast in prone position. This conflict requires estimating the relation between deformed and undeformed breast and applying the deformation to the three-dimensional speed of sound image. The deformation is simulated based on a biomechanical model using the finite element method. After simulation of the compression, the contours of the X-ray mammogram and the projected speed of sound image overlap congruently. The quality of the matching process was evaluated by measuring the overlap of a lesion marked in both modalities. Using four test datasets, the evaluation of the registration resulted in an average tumor overlap of 97%. The developed registration provides a basis for systematic evaluation of the new modality of three-dimensional speed of sound images, e.g. allows a greater understanding of tumor depiction in these new images.

Keywords: Registration, Ultrasound Tomography, Mammography, Image fusion

1. INTRODUCTION

Breast cancer is the most common type of cancer among women in Europe and North America.[1] In 2004, it was estimated that there were approximately 128,000 new cases of breast cancer and about 40,000 deaths caused by breast cancer in the United States.[2] Breast cancer is most effectively treated, if it is detected in an early stage since metastases are more likely to arise, when a tumor has grown over a long period of time.[3]

The established standard screening method is X-ray mammography. However, X-ray mammography frequently provides poor contrast for tumors located within glandular tissue and only produces two-dimensional projections of a deformed breast. Alternatively, MRI (Magnetic Resonance Imaging) is an established three-dimensional imaging method[4] which offers high contrast of soft tissue and high diagnostic accuracy. Additionally, the patient is not exposed to radiation. However, it is less specific and more expensive than X-ray mammography.[5]

A new approach is Ultrasound Tomography, which offers three-dimensional volumes of the breast in prone position. During the examination, the woman's breast is placed in a water bath. A ring-shaped ultrasound transducer surrounding the breast is translated downwards, recording multiple slice images of the breast. The transducer contains 256 bidirectional ultrasound elements. Because of the use of ultrasound, the patient is not subjected to radiation.

torsten.hopp@kit.edu, phone +49 7247 82-5990, adress: Hermann-von-Helmholtz-Platz 1, Eggenstein-Leopoldshafen 76344, Germany, http://www.ipe.kit.edu/

Medical Imaging 2010: Ultrasonic Imaging, Tomography, and Therapy, edited by Jan D'hooge, Stephen A. McAleavey,
Proc. of SPIE Vol. 7629, 762905 · © 2010 SPIE · CCC code: 1605-7422/10/$18 · doi: 10.1117/12.843454

Ultrasound Tomography provides three modalities: reflection images, attenuation images and speed of sound images.[6] Reflection images reveal changes in the echotexture and are therefore able to image the surface of tissues, resulting in a visualization of the morphology. Attenuation and speed of sound images are expected to show up mass lesions as high valued regions.[7]

Nevertheless, speed of sound images can not be compared directly to the standard screening method mammography, because of the difference in dimensionality and deformation. Hence, the quality of images can not be measured in comparison to mammography. The comparison is of interest for the evaluation of further clinical uses, as the Ultrasound Tomography is a technology in development. Since in future both modalities may complement each another, it will be of interest to combine the information for diagnosis.

The aim of this work is to develop a tool for evaluation of three-dimensional speed of sound images by automatically registering the images with the corresponding X-ray mammograms. The central problem in the registration is the large deformation of the breast during mammography. The breast has to be squeezed between two plates and is compressed up to 50% in diameter, which is nescessary for a good image contrast. This three-dimensional deformation is only recorded as two-dimensional projection. Hence, the individual three-dimensional deformation can not be obtained from these images. Additionally, the deformation of the breast depends on the individual positioning and shape of the patient's breast. Therefore, the exact projection angle, the amount of tissue imaged, the applied compression force and the thickness of the compressed breast are unknown.

In the following sections, we will present an automatic matching approach based on earlier works of Ruiter,[8] which performs the registration of X-ray mammograms and three-dimensional speed of sound images. The matching includes a patient-specific biomechanical model of the deformable behaviour of the breast to resolve the problem of the huge deformation during mammography. The model is described as Finite Element Model (FEM) and built based on the speed of sound image. The parameterization is carried out using information about the shape of the breast from the mammogram. It allows to simulate the deformation of the undeformed breast given in the speed of sound image to achieve a similar configuration as in a corresponding mammogram. The matching creates speed of sound projections directly comparable to the mammogram. The circumferences of the resulting images overlay congruently. Thus, for example the position of a suspicious lesion in the speed of sound image can be examined in the X-ray mammogram and the other way around (Figure 1).

In this paper, section 2 explains in detail the methodology of the registration approach. In section 3 we show first results with four clinical datasets. Finally section 4 concludes the paper and presents an outlook on current and future work.

2. METHODS

The challenge of this work is that X-ray mammograms show two-dimensional projections of a deformed breast, whereas speed of sound images render a three-dimensional undeformed breast. This conflict requires estimating the relation between deformed and undeformed breast and applying the deformation to the three-dimensional speed of sound image.

The deformation is determined by a compression simulation based on a patient specific biomechanical model of the breast. The model is built on the basis of the preprocessed and segmented speed of sound image and parameterized by the information of the mammogram. Afterwards the simulation of the deformation is carried out and the displacements are applied to the speed of sound image. The registration of the images of both modalities, is done after processing this step. The workflow of the matching process is illustrated in Figure 2. In the following subsections we present each step in more detail.

2.1 Preprocessing and segmentation

Both, the speed of sound image and the X-ray mammogram have to be preprocessed. In this first step, a software layer abstracts the loading of images of different formats, for example DICOM,[9] Image Stacks, RAW. Then the images are scaled and rotated to fit the internally used coordinate system. An interpolation is applied to the speed of sound image to overcome the possible gaps between the slices.

As the speed of sound varies only slightly between the surrounding water (around 1484 m/s at 20° C) and breast tissue (around 1540 m/s for fatty tissue), the contrast of this images is very low. The histogram of the

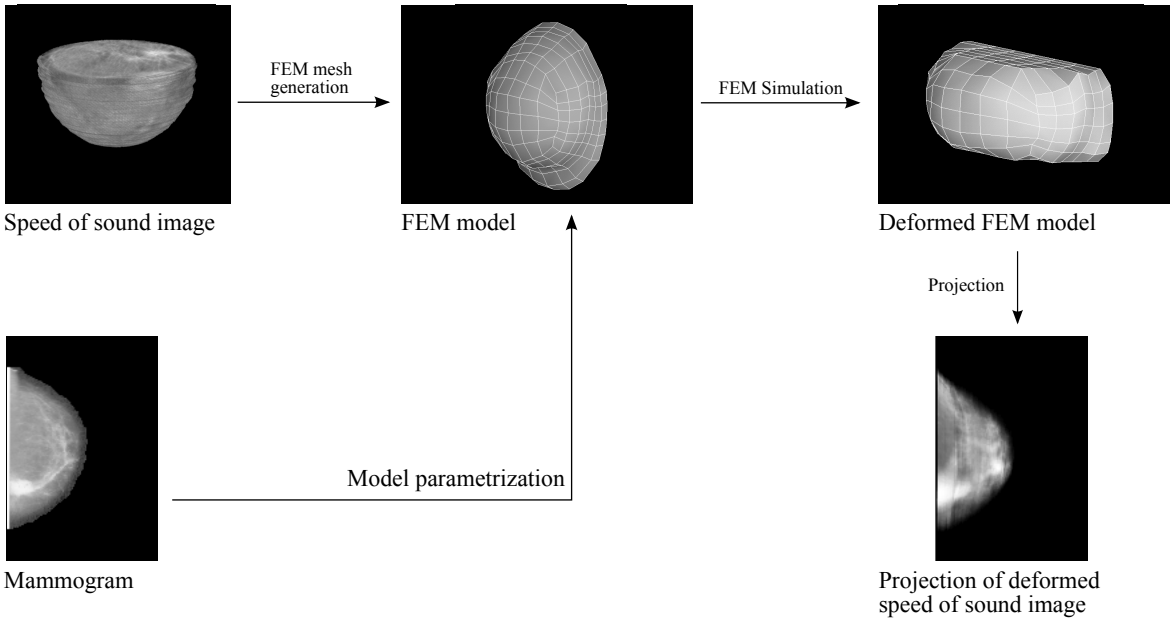

Figure 1: Principle of the matching of a speed of sound volume (top left) and the corresponding mammogram (bottom left). The speed of sound image is used to generate a FEM model. Information from the mammogram is taken to parameterize the FEM model, which is then subjected to a compression simulation. The resulting deformation is applied to the speed of sound image. Thus projection images can be carried out. The projection images overlay congruently with the corresponding mammogram.

speed of sound image is corrected to achieve a better contrast. These preprocessing steps are done in MATLAB,[10] therefore the MATLAB data format is used to store the preprocessed speed of sound images and mammograms.

In the second step, the image of each modality is segmented into background and object. For the mammogram and the speed of sound image, a presegmentation provided by the Karmanos Cancer Institute is used. Based on that, thresholding and morphological operations are used to smooth the segmentation mask.

2.2 Global Alignment

After preprocessing and segmentation, both images are passed to a global alignment method. The purpose of this method is to match the amount of breast tissue shown in the X-ray mammogram and in the three-dimensional speed of sound image, which may differ in both modalities. Furthermore, the specific projection angle of the X-ray mammogram is estimated.

To determine the amount of tissue imaged in both modalities, a two-dimensional projection of the speed of sound image is calculated, which is similar to the projection used in the corresponding X-ray mammogram. This requires the rotation of the speed of sound image by the angle given by the type of mammogram, cranio caudal or oblique. To match the contours of the X-ray mammogram, each row of the segmented breast in the speed of sound image is scaled to the width of the X-ray mammogram at its corresponding row. The speed of sound images used for the evaluation showed a smaller amount of tissue than the corresponding X-ray mammograms. In order to match the amount of tissue imaged in both modalities, the X-ray image is cropped iteratively and compared to the projection image of the speed of sound image. The quality of this comparison is determined using Normalized Mutual Information (NMI). The X-ray mammogram is then cropped at the position, which delivers the highest NMI value.

As the exact projection angle of the mammogram is not known, it has to be determined in a similar way to the automatic cropping described before. A projection of the speed of sound image is performed with projection angles ranging from -10° to +10° based on the angle given by the mammogram. For cranio caudal mammograms,

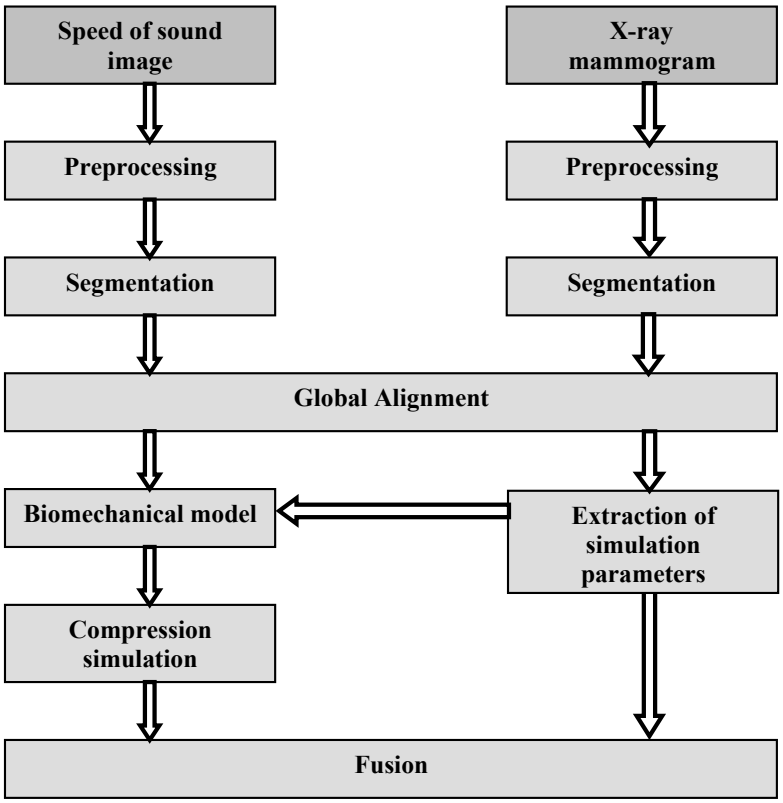

Figure 2: The matching process for X-ray mammograms and three-dimensional speed of sound images. Numerous processing steps have to be carried out: speed of sound images and X-ray mammograms have to be preprocessed and segmented. Afterwards a global alignment is done. Based on this and the segmented speed of sound image, a biomechanical model is built. Simulation parameters are extracted from the X-ray mammogram. Then the compression simulation is done, followed by the final step: the fusion of the images.

the estimated initial projection angle is 0°, for oblique mammograms, an angle of 45° is used initially for the projection. Each projection image is compared to the X-ray mammogram and their similarity is measured by NMI again. The projection angle which delivers the best NMI value is estimated to be the projection angle used during mammography.

2.3 Biomechanical model and compression simulation

In the next step, a patient specific biomechanical model is generated from the segmented three-dimensional speed of sound image to simulate the compression applied to the breast during mammography. Several deformation models for mammographic compression have been proposed in the literature. The Finite Element Method (FEM) is mostly used in advanced models since it simulates the physical behaviour of the breast.[8,11–15]

FEM is a method for the numerical solution of a physical problem described in a variational formulation. The basic idea of FEM is to divide the deformable body into finite elements, which are joined at discrete nodes. Aligning constraints are introduced at the connecting nodes to ensure the continuity of the model. The discretization is carried out by representing a desired function (displacement, stress or strain) within each element as a sum of element specific interpolation functions, the so-called shape functions.

For problems of solid mechanics, the deformation of a body can be approximated by the total potential energy. For small deformations and a linear elastic body, a linear approximation of the total potential energy Π of a body B can be by

$$\Pi(\{u\}) = \sum_{e=1}^{L} \left[\int_{B_e} \frac{1}{2} \{\epsilon\}^T \{\sigma\} dv - \int_{B_e} \{f\}^T \{u\} dv - \int_{S_{B_e}} \{t\}^T \{u\} ds \right]. \quad (1)$$

The first term on the right hand side is the total internal elastic strain energy. The second and third term are the potential energy of external volumetric and surface loads, in each case for one finite element B_e, with $e = 1, ..., L$. $\{\epsilon\}$ is the vector formulation of the Cauchy strain tensor, $\{\sigma\}$ is the vector formulation of the stress tensor. $\{f\}$ denotes the body forces and $\{t\}$ the surface tractions. With $\{u\}$, the displacement vector is formulated. dv denotes the volume of element B_e and ds the surface of an element S_{B_e}.

However, to model the mammographic deformation, geometric non-linearities have to be taken into account. Additionally, the deformation during mammographic compression is large. The Π of a body B subjected to large deformation in respect to the current configuration C^t can then be written as:

$$\Pi = \int_{B^{C^t}} \{\epsilon\}^T \{\sigma\} dv - \int_{B^{C^t}} \{f\}^T \{u\} dv - \int_{S_B^{C^t}} \{t\}^T \{u\} ds. \quad (2)$$

Small-step incremental solution methods are used to solve non-linear FE equation systems.

To describe the model of the breast, a meshing algorithm is needed. In the presented case we apply a surface oriented meshing, which uses the transfinite interpolation method.[16] It maps a unit cube to an arbitrary shaped volume. The boundaries of the unit template are mapped to the boundaries of the object. Then uniformly distributed nodes on the unit cube map to nodes on a mesh of the volume, where the curving of the mesh lines is influenced by the curving of the object boundaries.

As material model a neo-hookean material model is applied asuming only one tissue type in the breast. This is done according to Ruiter's experiments showing only slight differences when using a more complex model.[8] To obtain realistic compression forces, the material parameters suggested by Bakic[17] are used. They assume that the soft breast tissue is an incompressible material that consists mainly of water. Hence, for example, an applied deformation results only in a shape change, not in a change of the volume. The used model approximates the incompressibility with the typical FEM solution using a Poisson's ratio near 0.5.

To formulate the compression of the breast while recording the X-ray mammogram, boundary conditions for the FEM simulation are estimated and applied. Since the force applied in mammography is usually not recorded, the mammographic compression is mimicked by a two-step approach. In the first step, compression plates are added to the simulation. The deformation is carried out by moving the compression plates until a certain amount of compression is achieved (Figure 3). The thickness of the breast during mammography is estimated using the data given by the X-ray mammogram and the speed of sound image. This estimation is based on the assumption that the volume of the breast before compression equals the volume after compression. The shape of the breast is approximated by a semi-ellispoid described by the three axis diameters (x_n, y_n, z_n for the non-deformed breast, x_c, y_c, z_c for the compressed breast) of the breast. x_n, y_n and z_n are known by the segmented speed of sound image, x_c, z_c are know by the segmented mammogram. The only dimension not visible in any image is the thickness of the breast after compression (y_c). It is approximated as follows:

$$y_c = \frac{\frac{1}{2}\frac{4}{3}\pi\frac{x_n}{2}\frac{y_n}{2}\frac{z_n}{2}}{\frac{1}{2}\frac{4}{3}\pi\frac{x_c}{2}\frac{z_c}{2}} = \frac{x_n y_n z_n}{x_c z_c} \quad (3)$$

The compression plates of the first simulation are moved until the thickness of the biomechanical model between the plates equals the estimated thickness.

In the second step, the shape of the now deformed breast and the circumference of the corresponding mammogram are used to estimate the three-dimensional shape of the breast. The boundary conditions for this simulation are then formulated as displacements between the undeformed and deformed surface of the estimated three-dimensional shape (Figure 4). This results in a projection of the speed of sound image with exactly the same circumference as the segmented mammogram.

Formulated equations in the first and second step are solved using solution methods for large deformations in Ansys,[18] a commercial software to solve FEM simulations.

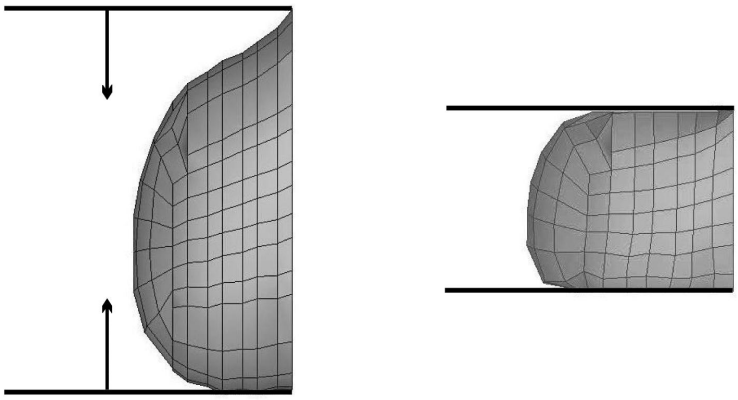

Figure 3: FEM simulation: biomechanical model of the breast before (left) and after (right) plate compression simulation.

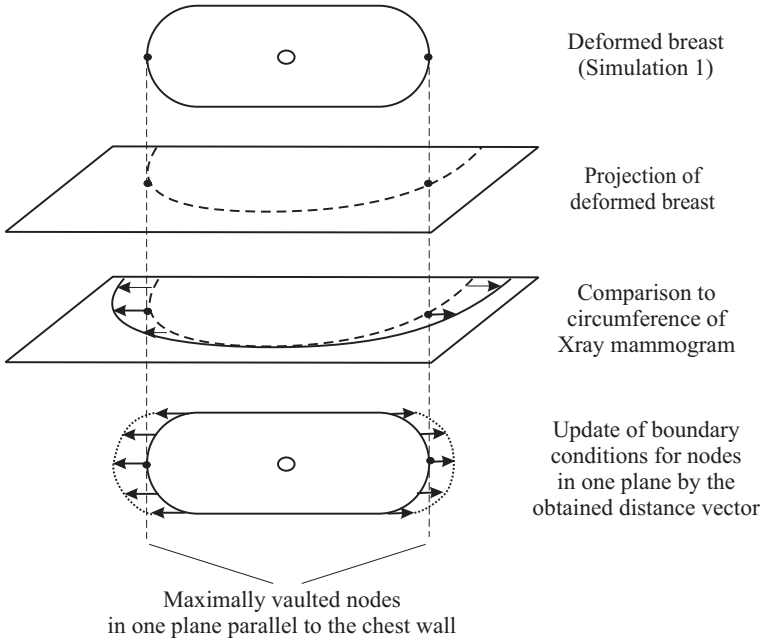

Figure 4: Compression simulation by updated boundary conditions.

2.4 Fusion

The final step is the creation of the registered projection of the speed of sound image. The deformation simulated by the FEM model is applied to the speed of sound image. Afterwards this deformed image is projected. The fusion is carried out using the nipple position to align both images in the frontal plane and the mean position of the chest wall to align them in the transversal plane. To be able to assign the location of a tumor in the three-dimensional speed of sound image directly to the X-ray mammogram, the resolution of the X-ray mammogram is reduced to equal that of the sound speed volume. Resulting images are directly comparable as their circumferences overlay congruently. Ideally, pixels with same coordinates show the same projected tissue of the breast.

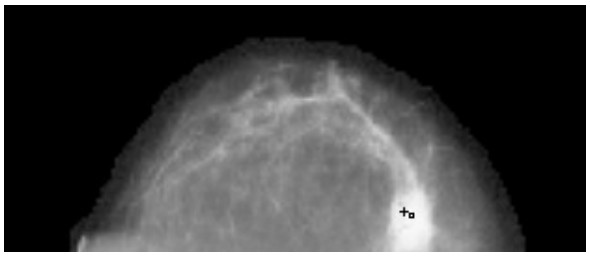

(a) X-ray mammogram (dataset 2). The center of the lesion in the X-ray mammogram is marked with a small rectangle, the center of the marked lesion after the deformation of the speed of sound image is marked with a cross. The distance between the centers is 3.8 mm.

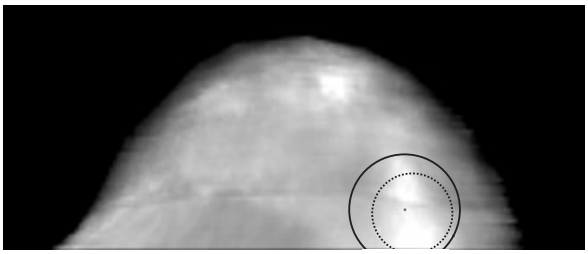

(b) Projection of the speed of sound image after compression simulation (dataset 2). The position of the lesion retrieved from the X-ray mammogram is marked as a dotted circle, the position of the lesion retrieved from the speed of sound image is marked as a solid circle. The overlap of the circles is 100%.

Figure 5: Resulting images of the registration of X-ray mammograms and speed of sound images.

3. RESULTS

The quality of the registration of the images can be estimated by the accuracy of the registration of lesions visible in both modalities. For this purpose, four datasets containing such lesions were provided by the Karmanos Cancer Institute. Each dataset consists of a speed of sound image and a X-ray mammogram of the same patient. The X-ray mammograms are analog mammograms with a resolution of 0.35 mm/pixel. The speed of sound images have a resolution of 1 mm/pixel with 70 slices at 221 x 221 pixel each. The medical findings show tumors in both modalities.

The segmentation of the images was generally very challenging, as the X-ray mammograms were low contrast scans of analog mammograms and the speed of sound images had low contrast of the breast surface.

For automatic generation of the patient specific finite element mesh, a smooth and accurate segmentation of the surface of the breast is necessary. The applied segmentation of the surface in the speed of sound images had to be corrected manually to obtain a valid Finite Element mesh. Also the circumferences of the mammograms were smoothed. These uncertainties in the surface and contour estimation contribute to the registration error. Additionally, the estimation of the automatic cropping to image the same amount of tissue is very sensitive to over- and underestimation of the segmented tissue. The automated cropping had to be corrected manually, the improvement of a more accurate and automated segmentation is subject to current research.

The biomechanical models created for the evaluation of the four datasets consist of 6^3 finite elements, each representing a material model mimicking glandular tissue.

The four datasets were reviewed by a radiologist and the centers as well as the circumferences of a lesion visible in both modalities were marked in both modalities. Hence, the simulated location of the lesion after deforming the speed of sound image and the real location retrieved from the mammogram can be compared as both images overlay exactly. By measuring the distance of the centers and the overlap of the circumferences between the lesion in the X-ray mammogram and in the projection of the deformed speed of sound image, the quality of the registration was estimated. The aim is a large overlap of the contours and a small deviation between real and estimated center position to be clinically applicable.

Resulting images are shown in Figure 5a respectively Figure 5b. Table 1 shows the evaluation results for the four datasets.

The mean displacement of the centers of the simulated and real location of the lesion is 7.3 mm (standard deviation 5.8 mm), the mean overlap is 97.5% (standard deviation 5.7%). However dataset 3 showed a highly deformed breast in the X-ray mammogram, which degrades the result. Aside from dataset 3, all datasets deliver very satisfying results. Hence, datasets 1, 2 and 4 are on a level to be suitable for clinical usage with an average overlap of these three datasets of 100% and a center distance of 4.4 mm.

Dataset	Overlap in %	Distance in mm
1	100	4.9
2	100	3.8
3	88.6	16.0
4	100	4.4

Table 1: Results of the evaluation of the registration of X-ray mammograms and speed of sound images.

4. CONCLUSION

To the best of our knowledge, a registration of three-dimensional speed of sound images and mammograms has not been carried out before. The presented method offers the possibility to compare two modalities directly. It takes into account that the deformation applied to the breast during mammography has to be applied to the three-dimensional data of the speed of sound images. In the future, our methodology can be used for systematic evaluation of the new imaging method.

The initial evaluation results are very promising. The average distance between the centers of the lesions in the projected speed of sound image and the X-ray mammogram is for most cases already acceptable and comparable to the results for MRI/X-ray registration shown by Ruiter.[8]

The presented method allows direct comparison of the standard screening method X-ray mammography with speed of sound images for systematic evaluation of the new three-dimensional imaging method. In a next step, the position of a tumor visible in both standard X-ray projections can also be localized in 3D in the speed of sound image of the undeformed breast.

After the evaluation of speed of sound images, the registration of these images may benefit clinical practice. The combined information, for example the high resolution of X-ray mammography and the expected good tissue characterization of the three-dimensional speed of sound images, can be used for multimodal diagnosis.

ACKNOWLEDGMENTS

This work is supported by the German Research Society under grant no. RU 1547/1-1

REFERENCES

[1] Fischer, T., Bick, U., and Thomas, A., "Mammographie-Screening in Deutschland," *Visions Journal* **15**, 62–67 (2007).

[2] American Cancer Society, "Cancer facts and figures 2008." Atlanta: American Cancer Society (2008).

[3] Sivaramakrishna, R. and Gordon, R., "Detection of breast cancer at a smaller size can reduce the likelihood of metastatic spread: A quantitative analysis"," *Academic Radiology* **4**(1), 8–12 (1997).

[4] Constantini, M., Magistrelli, A., and Franceschini, G., "MRI in phyllodes tumor of the breast. case reports," tech. rep., National center for Biotechnology Information (2002).

[5] Kaiser, W. A., Fischer, H., Vagner, J., and Selig, M., "Robotic system for biopsy and therapy of breast lesions in a high-field whole-body magnetic resonance tomography unit," *Investigative Radiology* **35**(8), – (2000).

[6] Duric, N., Littrup, P., Poulo, L., Babkin, A., Pevzner, R., Holsapple, E., Rama, O., and Glide, C., "Detection of breast cancer with ultrasound tomography: First results with the computerized ultrasound risk evaluation (C.U.R.E)," *Medical Physics* **34**(2), 773–785 (2007).

[7] Greenleaf, J. F. and Bahn, R. C., "Clinical imaging with transmissive ultrasonic computerized tomography," *Journal of Computer Assisted Tomography* **5**(5), – (1981).

[8] Ruiter, N. V., Stotzka, R., Mueller, T. O., Gemmeke, H., Reichenbach, J. R., and Kaiser, W. A., "Model-based registration of X-ray mammograms and MR images of the female breast," *IEEE Transactions on Nuclear Science* **53**, 204–211 (February 2006).

[9] National Electrical Manufacturers Association, "Digital imaging and communications in medicine (DICOM), DICOM standard,," (2008).
[10] The MathWorks Inc., "Matlab - the language of technical computing." http://www.mathworks.com/products/matlab/ (2009).
[11] Azar, F., *A Deformable Finite Element Model of the Breast for Predicting Mechanical Deformations under External Perturbations*, PhD thesis, University of Pennsylvania, USA (2001).
[12] Samani, A., Bishop, J., Yaffe, M., and Plewes, D., "Biomechanical 3-d finite element modeling of the human breast using mri data," *Medical Imaging, IEEE Transactions on* **20**, 271–279 (April 2001).
[13] Tanner, C., Degenhard, A., Schnabel, J. A., Castellano-Smith, A. D., Hayes, C., Sonoda, L. I., Leach, M. O., Hose, D. R., Hill, D. L., and Hawkes, D. J., "Comparison of biomechanical breast models: a case study," in [*Society of Photo-Optical Instrumentation Engineers (SPIE) Conference Series*], M. Sonka & J. M. Fitzpatrick, ed., *Presented at the Society of Photo-Optical Instrumentation Engineers (SPIE) Conference* **4684**, 1807–1818 (May 2002).
[14] Pathmanathan, P., Gavaghan, D., Whiteley, J., Brady, S. M., Nash, M., Nielsen, P., and Rajagopal, V., "Predicting tumour location by simulating large deformations of the breast using a 3d finite element model and nonlinear elasticity," *Medical Image Computing and Computer-Assisted Intervention MICCAI 2004* , 217–224 (2004).
[15] Ruiter, N., Zhang, C., Bakic, P., Carton, A., Kuo, J., and Maidment, D., "Simulation of tomosynthesis images based on an anthropomorphic software breast tissue phantom.," in [*Medical Imaging 2008: Visualization, Image-Guided Procedures, and Modeling (SPIE Proceedings Volume)*], Miga, M. I. and Cleary, K. R., eds. (2008).
[16] Knupp, P. and Steinberg, S., [*Fundamentals of Grid Generation*], CRC Press, Boca Raton, FL (1994).
[17] Bakic, P. R., *Breast tissue description and modeling in mammography*, PhD thesis, Lehigh University, USA (2000).
[18] Ansys Inc., "Software products." http://www.ansys.com.